Journal of Medicinal Chemistry Article

J. Med. Chem. **2009,** *52,* 6421–6432 **6421**
DOI: 10.1021/jm900914e

S-Glycosyl Primary Sulfonamides−A New Structural Class for Selective Inhibition of Cancer-Associated Carbonic Anhydrases

Marie Lopez,[†] Blessy Paul,[†] Andreas Hofmann,[†] Julia Morizzi,[‡] Quoc K. Wu,[‡] Susan A. Charman,[‡] Alessio Innocenti,[§] Daniela Vullo,[§] Claudiu T. Supuran,[§] and Sally-Ann Poulsen*[,†]

[†]*Eskitis Institute for Cell and Molecular Therapies, Griffith University, Nathan, Queensland 4111, Australia,* [‡]*Centre for Drug Candidate Optimisation, Faculty of Pharmacy and Pharmaceutical Sciences, Monash University, 381 Royal Parade, Parkville, Victoria 3052, Australia, and* [§]*Polo Scientifico, Laboratorio di Chimica Bioinorganica, Rm. 188, Università degli Studi di Firenze, Via della Lastruccia 3, 50019 Sesto Fiorentino, Florence, Italy*

Received June 21, 2009

In this paper, we present a new class of carbonic anhydrase (CA) inhibitor that was designed to selectively target the extracellular domains of the cancer-relevant CA isozymes. The aromatic moiety of the classical zinc binding sulfonamide CA inhibitors is absent from these compounds and instead they incorporate a hydrophilic mono- or disaccharide fragment directly attached to the sulfonamide group to give *S*-glycosyl primary sulfonamides (**1**−**10**). The inhibition properties of these compounds at the physiologically abundant human CA isozymes I and II and cancer-associated IX and XII were determined, and all compounds had moderate potency with K_is in the micromolar range. We present the crystal structures of anomeric sulfonamides **4**, **7**, and **10** and the sugar sulfamate drug topiramate in complex with human recombinant CA II. From these structures, we have obtained valuable insights into ligand−protein interactions of these novel carbohydrate-based sulfonamides with CA.

Introduction

Carbonic anhydrases (CAs,[a] EC 4.2.1.1) are zinc metalloenzymes that catalyze the reversible hydration of carbon dioxide to give bicarbonate and a proton: $CO_2 + H_2O \leftrightarrows HCO_3^- + H^+$. This reaction underpins cellular processes associated with respiration and transport of CO_2 and HCO_3^-, the provision of HCO_3^- for biosynthesis, the regulation of physiological pH, the secretion of electrolytes and fluids, as well as bone resorption and calcification.[1] In humans. 12 catalytically active CA isozymes (designated hCA, *h* = human) have been characterized and all 12 share a conserved active site topology that includes a tetrahedral Zn^{2+} cation coordinated to the side chains of three histidine residues, Figure 1. The Zn^{2+} core of CAs serves an essential function: it is a strong Lewis acid that binds to and activates the substrate water molecule. Hydration of CO_2 does not proceed at an appreciable rate under physiological conditions in the absence of CA.[1]

The modulation of CA activity has been validated as an avenue for the treatment of a range of acquired and inherited diseases.[1] Given the high degree of active site conservation among isozymes of CA, the enzyme class does however present a significant challenge as a drug discovery target. hCA isozymes I and II are widely distributed and have been known since the 1930s (with isozymes discriminated in the 1960s). Other hCA isozymes are much more recent discoveries, and interestingly they were characterized well after CA inhibitors were established as a mainstay of antihypertensive, antiglaucoma, antithyroid, and hypoglycemic drug treatment regimes. For example, the aromatic sulfonamide CA inhibitors acetazolamide, methazolamide, ethoxzolamide, and the bis-sulfonamide, dichlorophenamide, have been used clinically for over 40 years as CA inhibitors, Figure 2a.[1] Acetazolamide is the *par excellence* CA inhibitor and was the first nonmercurial diuretic to be used clinically commencing in 1956. The side effects of this "dirty" broad specificity CA inhibitor and other systemically administered CA inhibitors are now attributed to the inhibition of multiple CA isozymes throughout the body.[1] The primary sulfonamide ($-SO_2NH_2$) of these drugs binds to the active site Zn^{2+} of CAs (Figure 2b) and blocks access to the zinc coordination sphere for the substrate water molecule, thus impeding the hydration of CO_2.[1]

The optimization of molecular recognition interactions between ligand and enzyme is an important approach for increasing the potency of a ligand, however in isolation this approach is insufficient when the primary goal of our research efforts is to develop useful drug-like compounds.[2] Drug design must take into account the relevant biological landscape for both normal and diseased cells/tissues associated with the drug target. While different hCA isozymes have a high degree of active site conservation, the isozymes have variable tissue distribution, subcellular locations, and expression profiles,[1] and it is these differentiating properties that underpin added opportunities for medicinal chemistry programs to target CA isozymes selectively. This strategy should

*To whom correspondence should be addressed. Phone: +61 7 3735 7825. Fax: +61 7 3735 7656. E-mail: s.poulsen@griffith.edu.au.

[a] Abbreviations: CA, carbonic anhydrase; TPM, topiramate; P_e, effective permeability; pH_e, extracellular pH; pH_i, intracellular pH; PAMPA, parallel artificial membrane permeability assay; PVDF, polyvinylidene fluoride; DOPC, dioleoyl-3-phosphocholine; c LogP, calculated Log P; TPSA, total polar surface area; ELSD, evaporative light scattering detection.

Published on Web 09/30/2009

limit polypharmacology and result in therapeutics with improved tolerability, safety, and efficacy.[2] A successful example of this approach was the pursuit and clinical launch of aromatic sulfonamides as topically acting antiglaucoma agents, namely dorzolamide (Merck & Co., 1995) and brinzolamide (Alcon Laboratories, 1998), Figure 3.[3,4] These compounds are potent inhibitors of hCA II within the ciliary processes of the eye and are used clinically to reduce intraocular pressure, which is the key physiological dysfunction presenting in patients with glaucoma. Topical administration avoids many of the side effects associated with earlier used orally administered CA inhibitor-based drugs by selectively targeting CAs in the eye tissue. The success of these compounds in the market is testament to the principle that efficacious CA inhibitors can provide safer and well tolerated treatments when they act with specificity.

The historically broad pharmacological footprint of CA inhibitors together with our modern day understanding of the chemical biology of CA isozymes underpins opportunities for the development of new CA-based therapies. An important recent finding in CA research has been the validation of hCA IX and XII as therapeutic targets for cancer chemotherapy intervention.[5,6] A phenotype of solid tumors is an acidic microenvironment (low pH_e) caused by heightened metabolism that leads to an elevated level of both secreted lactic acid and CO_2, which when combined with poor clearance (owing to inadequate vasculature around the solid tumor) leads to increased extracellular acidity.[6,7] While low pH_e promotes tumor growth and development, a variation to intracellular pH (pH_i) represents a severe threat to cancer cell survival through disruption of critical biological functions.[6,7] Cancer cell survival thus depends on both low pH_e with a concomitant need for (normal) physiological pH_i. Pouysségur and colleagues recently demonstrated that expression of CA IX and XII grants hypoxic tumor cells a survival advantage, as these enzymes regulate and maintain pH_i levels that support cellular functions.[6] Transcriptional activation of the ca9 and ca12 genes in hypoxic tumor cells is regulated by hypoxia-induced factor 1 (HIF-1).[8] The results of in vivo studies in mice showed that silencing of ca9 and ca12 genes significantly reduced the rate of xenograft growth. A 40% reduction in xenograft tumor volume occurred with ca9 silencing and a dramatic 85% reduction with invalidation of both ca9 and ca12; this outcome is attributed to slowed proliferation in the absence of extracellular CA.[6] Several research groups have provided validation that specific targeting of CA IX (or IX and XII) may lead to an effective anticancer therapy, particularly for the benefit of patients with hypoxic tumors.[5−7] As a candidate for drug intervention CAs possess two discriminating attributes that provide opportunities for selective targeting with small molecule inhibitors. First, hCA IX expression in hypoxic tumors occurs within tissues that normally lack this isozyme such as carcinomas of the lung, breast, esophagus, cervix, and kidney.[9] Second, unlike the physiologically dominant cytosolic hCA I and hCA II, hCA IX and XII are transmembrane proteins with an extracellular enzyme active site. It has been demonstrated already that hCA IX and XII display high affinity for primary aryl and heteroaryl sulfonamides[10,11] and that their inhibition can reverse the acidification of the tumor microenvironment and retard tumor growth.[9] The validation of these extracellular domains as cancer therapy targets has flagged an urgent need for the development of cell impermeable CA inhibitors that specifically act on these

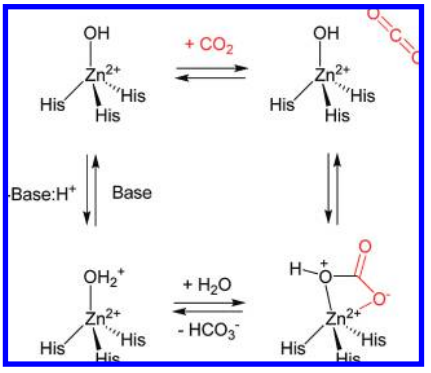

Figure 1. Schematic of the CA active site catalytic cycle that is common to all catalytically active human CA isozymes. The zinc cation is an excellent Lewis acid and is bound to three histidine residues and the substrate water molecule. This Zn^{2+}coordinated water has a pK_a of ~7.[1] CA thus facilitates deprotonation of water at physiological pH to generate the strongly basic hydroxide anion (OH^-), which is the reactive species in the hydration of CO_2 leading to formation and release of HCO_3^-.

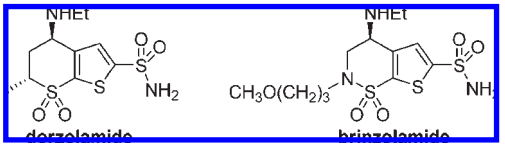

Figure 3. Dorazolamide and brinzolamide are topically administered CA inhibitors that are used clinically to lower intraocular pressure in patients with glaucoma.

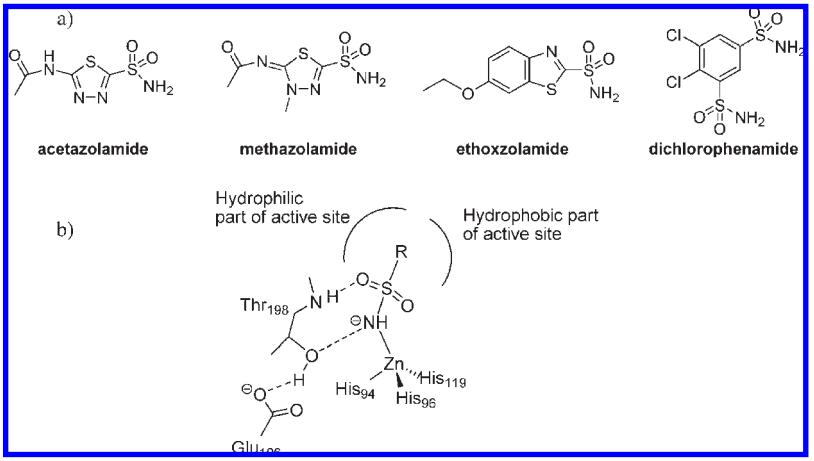

Figure 2. (a) Systemically administered CA inhibitors. All have a primary sulfonamide group as the zinc binding function. (b) CA active site schematic of sulfonamide mediated inhibition ("canonical binding mode").

membrane-associated CAs for use as tools or lead molecules for cancer therapy and/or diagnostics discoveries.[6,7]

In the past few years, our group has developed a medicinal chemistry program to differentiate inhibition of transmembrane CAs from cytosolic CAs.[12−17] Our approach has been to tether a carbohydrate moiety to the high-affinity aromatic sulfonamide CA pharmacophore, leading to sulfonamide glycoconjugates with a sugar-aromatic-SO_2NH_2 motif. Mounting evidence supports the premise that sugar-based molecules have value as drug candidates, as they often present desirable activity and safety profiles.[18−20] The $-SO_2NH_2$ zinc binding function of the glycoconjugates, as for other CA inhibitors, facilitates a critical role in enzyme recognition and is essential for efficacy. The role of the sugar is however to facilitate selective or preferential inhibition of transmembrane CAs over cytosolic CAs, as this hydrophilic moiety impairs the ability of the sulfonamide glycoconjugates to passively diffuse through lipid membranes.[12] The stereochemical and structural variability of the carbohydrate moiety also provides the opportunity for interrogation of subtle differences of active site architecture among different CA isozymes. Our approach thus provides neutral and water-soluble CA inhibitors that have excellent potential as isozyme selective inhibitors as a consequence of tuning physicochemical properties.[12−17]

Recently, one of our groups reported the synthesis of *S*-glycosyl primary sulfonamides, a new class of compound wherein a primary sulfonamide moiety is directly attached to the anomeric center of a mono- or disaccharide fragment.[21] Therein we disclosed novel synthetic methodology to access a new chemical class that had so far proven elusive to chemical synthesis. At the same time as our paper was published, Somsák reported an alternate synthesis to similar compounds.[22] As new chemical entities that incorporate the classical zinc binding primary sulfonamide function coupled directly to a sterochemically rich carbohydrate scaffold (that is, without an intervening aromatic moiety), we were interested in investigating this novel sugar-SO_2NH_2 motif for CA inhibition. Herein we present the inhibition profile of a panel of anomeric sulfonamides (compounds **1**−**10**) against the cancer associated (hCA IX and XII) and physiologically dominant (hCA I and II) carbonic anhydrase isozymes. The novelty of the anomeric sulfonamide structural motif together with the inhibition data acquired has led us also to pursue protein X-ray crystallography to identify the structural features of these molecules within the active site of hCA II that are important for the observed enzyme inhibition profile. We also investigate the membrane permeability properties of these carbohydrate-based CA inhibitors to evaluate the potential of the lipid membrane barrier as a means toward selectively targeting small molecule CA inhibitors to the extracellular cancer-associated isozymes IX and XII.

Results and Discussion

Chemistry. A set of 10 *S*-glycosyl primary sulfonamides **1**−**10** (Figure 4) were synthesized from per-*O*-acetylated sugar derivatives as outlined in Scheme 1 and described by us previously.[21] Our general approach to the synthesis consists of first introducing a thioacetate group at the anomeric center of a per-*O*-acetylated sugar derivative. From this follows formation of a *NH*-dimethoxybenzyl (DMB) glycosyl sulfenamide, oxidation of this sulfenamide to give a glycosyl *NH*-DMB sulfonamide, and removal of the DMB sulfonamide protecting group to yield a primary sulfonamide at the anomeric center. Target sugars were prepared either as per-*O*-acetylated (**1**−**5**) or fully deprotected (**6**−**10**) anomeric sulfonamides. The chemistry was applied to a variety of monosaccharides: D-glucose (→**1** and **6**), D-galactose (→**2** and **7**), and D-glucuronic acid methyl ester (→**3** and **8**) and disaccharides lactose (→**4** and **9**) and maltose (→**5** and **10**).

Carbonic Anhydrase Inhibition. Enzyme inhibition data was determined for physiologically dominant hCA I and II and cancer-associated hCA IX and XII by assaying the CA catalyzed hydration of CO_2.[23] Inhibition and isozyme selectivity ratio data for the anomeric sulfonamides **1**−**10** as well as for the standard CA inhibitor acetazolamide, the sugar sulfamate drug topiramate, and the aliphatic sulfonamide drug zonisamide are presented in Table 1. The structures for topiramate and zonisamide are in Figure 5.

The majority of clinically relevant CA inhibitors possess a flat aromatic moiety with a bland stereochemical profile.[1] In this type of inhibitor, the sulfur atom of the primary

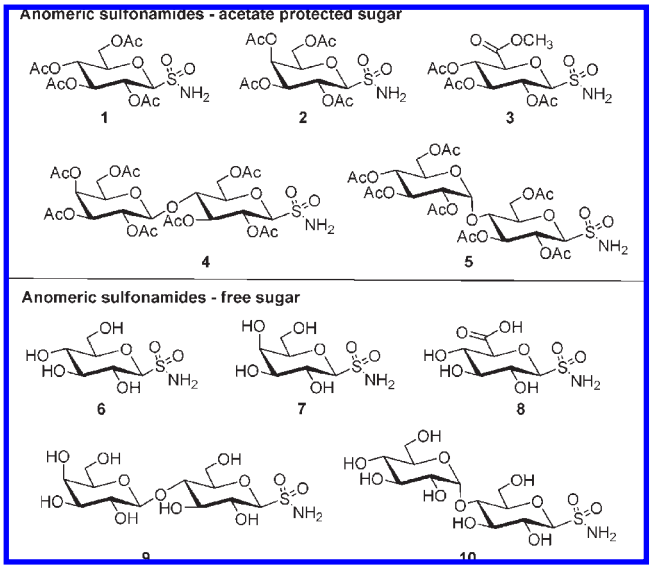

Figure 4. Target anomeric sulfonamide compounds: per-*O*-acetylated derivatives (**1**−**5**) and fully deprotected derivatives (**6**−**10**).

Scheme 1. Synthesis of *S*-Glucosyl Primary Sulfonamides **1** and **6** from per-*O*-Acetylated D-glucose[a]

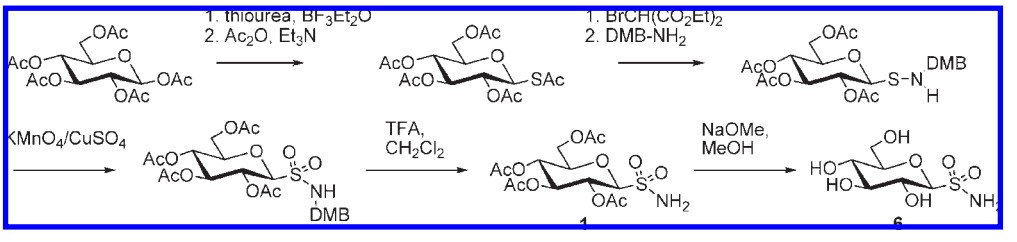

[a] Compounds **2**−**4** and **7**−**10** were synthesized similarly from per-*O*-acetylated sugar precursors.[21]

Table 1. Inhibition and Isozyme Selectivity Ratio Data of hCA Isozymes I and II (Cytosolic), IX and XII (Tumor-Associated) with Anomeric Sulfonamides **1**−**10**, and the Established Drugs and CA Inhibitors Acetazolamide, Topiramate, and Zonisamide

	K_i (μM)[a]				selectivity ratios[b]	
compd	hCA I[c]	hCA II[c]	hCA IX[d]	hCA XII[d]	hCA I/ hCA IX	hCA II/ hCA IX
acetazolamide	0.25	0.012	0.025	0.0057	10	0.48
topiramate	0.25	0.005	0.058	0.0038	4.3	0.09
zonisamide	0.056	0.035	0.005	11	11.2	7.0
1	4.53	4.50	3.91	4.66	1.16	1.15
2	3.92	4.73	4.09	4.75	0.96	1.16
3	4.34	4.35	4.15	4.71	1.05	1.05
4	4.68	4.51	4.03	4.60	1.16	1.12
5	4.12	4.98	4.08	4.61	1.01	1.22
6	3.90	4.91	4.05	4.69	0.96	1.21
7	3.93	4.55	4.19	4.80	0.94	1.09
8	3.71	3.90	3.95	4.55	0.94	0.99
9	3.97	3.92	4.19	4.77	0.95	0.94
10	4.15	4.10	4.22	4.84	0.98	0.97

[a] Errors in the range of ±5−10% of the reported value from three determinations. [b] The K_i ratios are indicative of isozyme selectivity in vitro. [c] Human (cloned) isozymes. [d] Catalytic domain of human (cloned) isozymes.

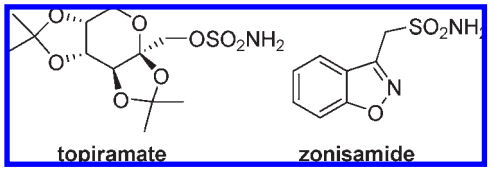

Figure 5

sulfonamide zinc anchor group is directly bonded to a sp^2 hybridized carbon atom, Figure 2a. Sulfonamide derivatives such as the isosteric sulfamates and sulfamides are also well-known CA inhibitors.[24,25] In these compounds, the sulfonamide sulfur atom is attached to an electronegative atom: oxygen for sulfamates (R-O-SO_2NH_2)[26] and nitrogen for sulfamides (R-NH-SO_2NH_2).[27−29] Topiramate, a fructopyranose sulfamate, is a billion dollar drug that is marketed worldwide for the treatment of epilepsy and migraine.[30,31] This compound has been shown to be a good inhibitor of CAs in vitro by a stopped flow technique monitoring the physiological reaction catalyzed by these enzymes, i.e., CO_2 hydration to bicarbonate and protons.[25] The chemical structure of this carbohydrate-based sulfamate (Figure 5) is particularly notable from the point of view that its structure is in stark contrast to the bland sterochemical motif of many known CA inhibitors and hence draws some interesting parallels with the new chemical entities presented in this study, and we will discuss these further later in this manuscript. There are also examples, albeit more limited, of sulfonamides as CA inhibitors wherein the sulfonamide sulfur is directly attached to a sp^3 hybridized carbon to give a methylene sulfonamide motif (R-CH_2-SO_2NH_2). These compounds also present as potent CA inhibitors, and an example of this inhibitor class is the antiepileptic drug zonisamide, Figure 5.[32] Both topiramate and zonisamide have a complex biological effect, which may or may not include CA inhibition in the mechanism of action. Irrespective, these compounds are structurally novel CA inhibitors when compared to the typical aromatic sulfonamides, and as clinically used drugs they have passed the many hurdles that small molecules face through the drug development pipeline, and hence may serve as a valuable comparative chemical tools for the current study of anomeric sulfonamides. To the best of our knowledge, there are no compounds with a methine sulfonamide motif (RR′-CH-SO_2NH_2) for which a CA inhibition response is available—the anomeric sulfonamides herein belong in this unreported class.

Acetazolamide and topiramate exhibit similar CA inhibition profiles. Both are low nanomolar inhibitors of hCA II and XII (K_is 3.8−12 nM), slightly weaker inhibitors of hCA IX (K_is 25−58 nM), and less potent inhibitors of hCA I (K_is both 250 nM). Zonisamide is a very potent inhibitor of hCA IX (K_i of 5.1 nM), a mid-potency inhibitor of hCA I and II (K_is 35−56 nM), and a weak inhibitor of hCA XII (K_i of 11 μM). In contrast to standard CA inhibitors, the inhibition profile for the anomeric sulfonamide compounds **1**−**10** is flat and there is no variation in the K_i values observed across all CA isozymes investigated, leading to K_i selectivity ratios of ∼1.0 across isozymes, i.e., they are nonselective CA inhibitors. Neither the stereochemistry presented by the differing sugar moiety nor the nature of the sugar hydroxyl groups, either as the polar free sugar (sugar−OH, **6**−**10**) or less polar and bulkier acetylated sugar (sugar−OAc, **1**−**5**) impacted to alter enzyme inhibition characteristics. At the physiologically dominant isozymes K_is were 3.71−4.68 μM at hCA I and 3.90−4.98 μM at hCA II, while at the cancer-associated isozymes, K_is were 3.91−4.22 μM at hCA IX and 4.55−4.84 μM at hCA XII. This flat SAR and micromolar CA inhibition represents an anomaly in our drug discovery program wherein to date the "norm" has been to readily prepare CA inhibitors that display nanomolar inhibition constants similarly to many known sulfonamide-based CA inhibitors. These atypical inhibition results prompted us to turn our attention to a structure-based investigation of the anomeric sulfonamides with hCA II. Using this structure-based approach, we planned to discern the interactions of our compounds with active site residues of hCA II so as to identify the structural features of these ligands that are responsible for the weaker micromolar inhibition observed. The sugar sulfamate topiramate has a structural motif that is related to that of the anomeric sulfonamides **1**−**10**, as each are based on natural product sugar scaffold, a zinc binding function, and lack an aromatic moiety. Topiramate is a good hCA II inhibitor (K_i of 5 nM), whereas for the anomeric sulfonamides **1**−**10**, K_is were 3.90−4.98 μM, i.e., approximately 3 orders of magnitude weaker inhibitors than topiramate. We specifically targeted protein X-ray crystallography to enable comparison of the active site binding attributes of the new ligands with those of topiramate in the hCA II active site. We also attempted to find clues as to potential ligand interactions with hCA IX using a homology model of the catalytic domain of this membrane-bound

Table 2. Data Collection and Structure Refinement Statistics of Ligand-Bound hCA II Crystal Structures

ligand data set	**4** hCA II:**4**	**7** hCA II:**7**	**10** hCA II:**10**	topiramate hCA II:**TPM**
		Data Collection		
X-ray source	AS-PX1	AS-PX1	in-house	in-house
wavelength (Å)	0.9568	0.9568	1.5418	1.5418
space group	$P2_1$	$P2_1$	$P2_1$	$P2_1$
cell parameters (Å; deg)	42.4, 41.7, 72.5; 104.5	42.5, 41.7, 72.5; 104.5	42.4, 41.7, 72.5; 104.9	42.3, 41.4, 72.4; 104.6
resolution (Å)	1.8	1.8	2.4	1.8
multiplicity	7.5 (7.3)	7.5 (7.5)	3.5 (3.1)	3.3 (3.2)
completeness (%)	99.5 (96.9)	99.9 (100)	99.3 (95.5)	99.8 (98.7)
R_{merge}	0.055 (0.287)	0.062 (0.558)	0.053 (0.160)	0.033 (0.058)
		Structure Refinement		
no. of water molecules	93	87	164	354
average *B* actor (Å^2)	23.8	24.2	14.9	16.6
rms bond lengths (Å)	0.005	0.005	0.018	0.013
rms bond angles (deg)	1.436	1.340	1.782	1.368
rms bonded *B* factors (Å^2)	2.9	2.5	1.6	1.5
Ramachandran plot (%)[a]	88.4, 11.1, 0.5, 0	88.0, 11.6, 0.05, 0	84.9, 14.2, 0.9, 0	88.0, 11.5, 0.5, 0
R factor	0.196	0.200	0.154	0.153
R_{free}	0.220	0.220	0.247	0.198
		Ligand		
average *B* factor (Å^2)	59.5	28.2	33.5	12.2
hexose ring 1/ring 2 (Å^2)	49.9/69.5	n/a	22.3/34.1	n/a

[a] Residues in most favored regions, additional allowed regions, generously allowed regions, disallowed regions.

enzyme. Because of the high degree of conservation of residues within the active site, no significant differences in ligand−protein interactions could be identified. Currently, there is no crystal structure available for hCA IX, however recently a structure of a hCA IX active site mimic that is a double mutant of hCA II was reported.[33]

Structures of hCA II:Ligand Complexes. To obtain insights into ligand−protein interactions at the atomic level, we attempted determination of crystal structures of human recombinant CA II in complex with ligands **1**−**10** as well as topiramate. Using cocrystallization as well as soaking techniques, not all ligands were found to be present in the crystals examined. With cocrystallization, crystal structures of hCA II in complex with one monosaccharide (**7**), two disaccharides (**4** and **10**), and topiramate were obtained. Data collection and refinement statistics are presented in Table 2.

The vast majority of publications on drug discovery targeting hCA II annotate residue numbers in the active site that are offset by one relative to the amino acid sequence of hCA II. This may be a consequence of the numbering scheme used in the early hCA II crystal structures (PDB codes 1CA2, 2CBB), which skip residue number 126. In this study, we have applied a residue numbering scheme that is in accordance with the amino acid sequence of hCA II.

As expected, the binding mode of the sulfonamide (or sulfamate) moiety to the catalytic zinc ion is invariant, and all four ligands share the binding mode depicted in Figure 2b. The crystal structure of hCA II:topiramate is in excellent agreement with the previously published structure of this ligand in complex with hCA II.[25] All ligands investigated in this study occupy space in the active site cleft of hCA II without altering the configuration of residues lining the active site (see Table 3, Figure 6). Notably, even topiramate with its rather oblate shape is not causing a significant change in configuration of active site residues.

In addition to the canonical sulfamate interactions (Figure 2b), the topiramate sugar moiety also interacts with

Table 3. Comparison of Active Site Residue Configuration of Apo- and Ligand-Bound Structures of hCA II[a]

	reference structure	
comparison structure	apo-hCA II (PDB: 1CA2) positional rms (Å)	hCA II:**TPM** positional rms (Å)
hCA II:**4**	0.151	0.266
hCA II:**7**	0.133	0.238
hCA II:**10**	0.177	0.233
hCA II:**TPM**	0.244	

[a] The positional root mean square deviation of 22 residues lining the active site was calculated for all 184 atoms using the program Align.[34]

the side chains of Asn62, Gln92, and Thr199 through direct hydrogen bonds, while Ala65 and Phe130 provide hydrophobic contacts to the aliphatic parts of the two isopropylidene moieties, Figure 7, Table 4. The crystal structures of the three anomeric sulfonamide ligands reveal the conservation of a hydrogen bond with the side chain of Thr199 and a hydrophobic contact with Leu197, Figure 7 and Table 4. Despite the complexity of disaccharides **4** and **10**, these ligands are not able to form as many direct interactions with protein residues as topiramate. Compounds **10** and **7** show indirect interactions of their free hydroxyl groups with protein side chain residues through a network of ordered water molecules. Poor electron density was observed for the distal hexose ring of disaccharides **4** and **10** as well as for several of the acetyl moieties of **4**, indicating that the ligands are not well ordered in the active site cleft. This observation is also consistent with the thermal displacement factors of the ligand atoms of data sets hCA II:**4** and hCA II:**10**, Table 2. For the data sets reported here, there was no ambiguity as to the presence of ligands in the active site cleft because the initial electron density clearly allowed us to distinguish between cases where water, sulfate anion, or sulfonamide was bound to the catalytic zinc ion, Figure 8.

Both topiramate and the anomeric sulfonamides of the kind presented in this study possess a central carbohydrate skeleton and present various functional groups that

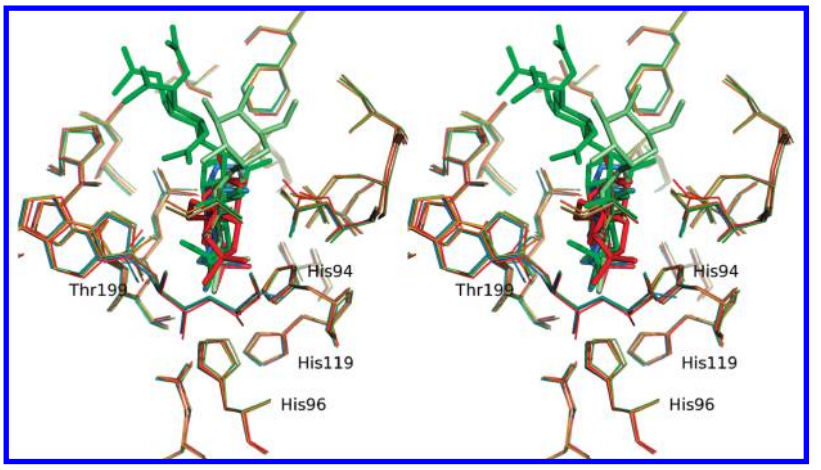

Figure 6. Comparison of ligand and active site residue configurations. The four ligand-bound structures of hCA II determined in this study (**4**, green; **10**, pale green; **7**, blue; topiramate, red) are superimposed on the structure of apo-hCA II (PDB: 1CA2; orange). The 22 residues lining the active site of hCA II are shown as wireframe, ligands are drawn as stick models. The stereo figure was prepared with PyMOL.[35]

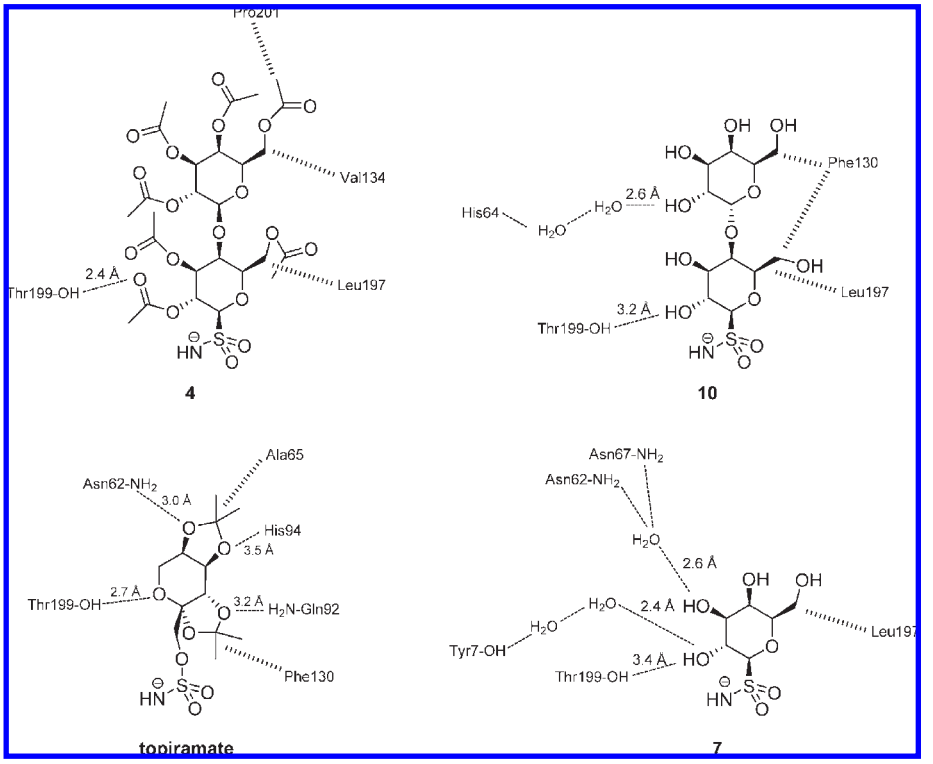

Figure 7. Schematic view of ligand interactions with protein residues in hCA II:ligand crystal structures. The canonical sulfonamide and sulfamate interactions (Figure 2b) are not shown for the purpose of clarity.

Table 4. Summary of Ligand Interactions with Protein Residues in hCA II:Ligand Complex Crystal Structures[a]

ligand	**4**	**10**	**7**	topiramate
direct hydrogen bonds	1	1	1	4
H_2O hydrogen bonds	0	1	2	0
vdW interactions	3	3	1	2

[a] The canonical sulfonamide and sulfamate interactions are not included.

potentially could interact with protein residues. A key structural difference we have identified between the anomeric sulfonamides and topiramate is the overall shape of these molecules. Topiramate presents a "T" shaped ligand with the sugar moiety and its two isopropylidine hydroxyl protecting groups neatly plugging the hCA II active site anchored by the

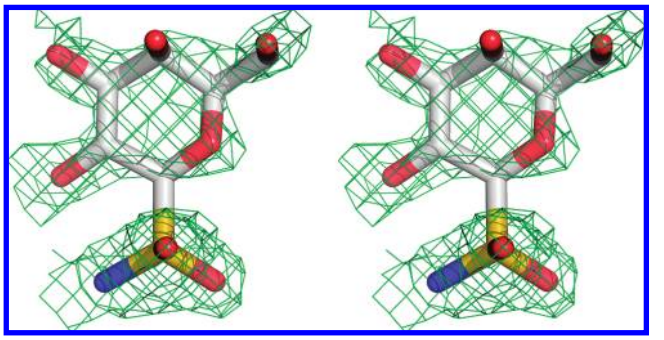

Figure 8. Initial difference electron density of hCA II:**7** contoured at 1.8σ. The density features allowed unambiguous placement of the hexose ring. Stereo figure prepared with PyMOL.[35]

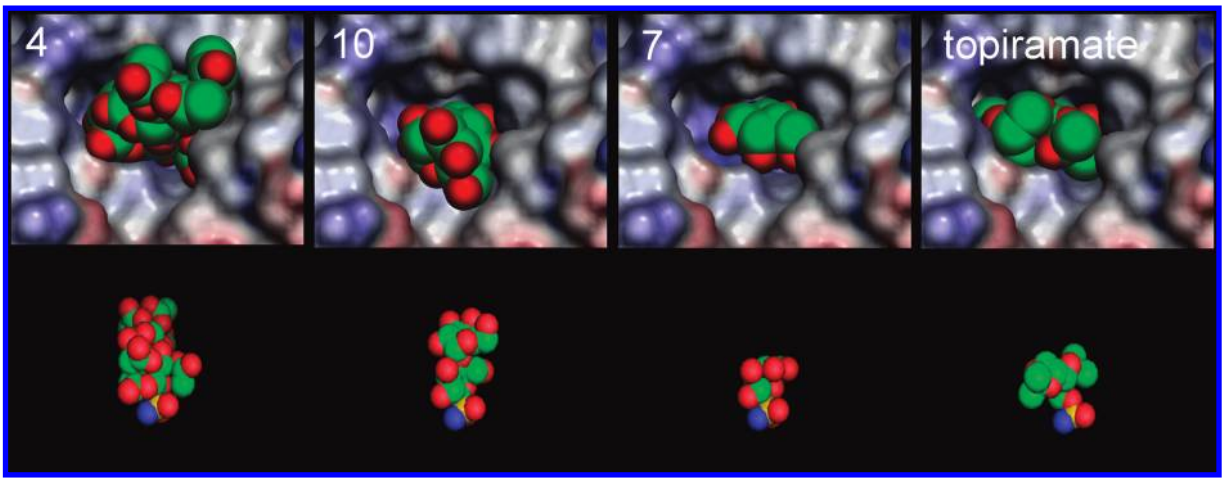

Figure 9. Comparison of ligand shapes. Shape complementarity between ligands and active site of hCA II. The ligand atoms are shown as spheres and the protein surface is colored by electrostatic potential. Upper panel figures prepared with AstexViewer.[36] All ligands of lower panel are shown in their superimposed, protein-bound conformations and rendered as sphere models. Lower panel figures prepared with PyMOL.[35]

zinc binding sulfamate group. The diisopropylidine sugar moiety effectively spans the diameter of the conical shaped active site cleft at a height of about 5 Å above the catalytic zinc ion, enabling a total of six direct interactions with the protein (Table 4, Figure 9). In contrast, the anomeric sulfonamide compounds tested in this study present an elongated rather than "T" shaped ligand. The sugar moieties of these ligands do not provide sufficient transverse bulk to span the active site cleft as for topiramate, Figure 9. This shape difference leads to a high degree of flexibility of ligand conformations in the protein-bound state and to less than optimal active site occupancy, exemplified through weaker and fewer interactions of the inhibitor with the enzyme active site, Table 4 and Figure 9.

Comparison with hCA IX Active Site. Using a homology model of hCA IX (90−341), potential interactions of compounds **4**, **7**, **10**, and topiramate were assessed. The constitution of the active site of hCA IX is highly similar to that of hCA II as far as amino acid sequence identity is concerned. Comparing the two active sites, only eight residues are substituted, mostly in a conservative fashion: Glu69/Thr155, Leu60/Arg146, Ile91/Leu173, Ala65/Ser151, Asn67/Gln153, Phe130/Val212, Val134/Leu216, Leu203/Ala287. Out of these, only Ala65/Ser151 and Asn67/Gln153 are of practical interest because the other substitutions occur in the periphery and at the top of conical active site cleft.[33] The substitution of Asn67 with Gln153 in case of hCA IX does not introduce new functionality in this area but may allow interactions with a ligand situated in the center of the cleft due to spacer arm being longer by one methylene unit. Ser151, substituting for Ala65 of hCA II, may be more within the interaction radius of the core structure of a ligand. When comparing the structures of **4**, **7**, and **10** bound to hCA II with the homology model of hCA IX by means of superposition, it is obvious that none of the compounds explores the active site space to an extent that would utilize interactions with Ser151 or Gln153. Interestingly, when superimposing our hCA II:topiramate structure with the hCA IX homology model, one of the isopropylidene units of this ligand clashes with Ser151, which may explain the lower inhibition of topiramate for hCA IX (see Table 1).

Passive Membrane Permeability. In the development of anticancer compounds that target hCA IX and XII knowledge about passive diffusion across biological membrane barriers is crucial. We[13−17] and others [37−41] have adopted a strategy to deliberately manipulate physicochemical properties so as to impart membrane impermeability into the CA small molecule inhibitor. So far, few studies have interrogated the effectiveness of this design strategy with a quantitative assessment of membrane permeability.[38,39]

In general, passive diffusion across biological membrane barriers is related to the lipophilicity of the small molecule and permeability generally decreases with increasing polarity or capacity for hydrogen bonding. Log *P* represents intrinsic lipophilicity and compounds with Log $P < 0$ typically have good solubility but poor lipid bilayer permeability (although paracellular permeability may be a contributor for very small hydrophilic molecules).[42] In this study, we have calculated the theoretical cLog P for the anomeric sulfonamides as well as the standard CA inhibitors acetazolamide, topiramate, and zonisamide, Table 5. The anomeric sulfonamides **6**−**10** are hydrophilic, with cLog Ps that range from −2.8 for the monosaccharides (four free hydroxyl groups) to −5.0 (disaccharides with seven free hydroxyl groups). The cLog P values for the acetylated sugars **1**−**5** are consistent with the incorporated acetate groups, decreasing the polarity of the resulting sugar moiety, with cLog Ps that range from −0.6 for the monosaccharides (four acetate groups) to −0.2 for disaccharides (seven acetate groups). Although compounds **1**−**5** are several log units less negative than **6**−**10**, their cLog P values still fall within the range indicative of molecules with poor membrane permeability, i.e., Log $P < 0$.

Another small molecule property that has been shown to be a descriptor for characterizing lipid membrane barrier diffusion is topological polar surface area (TPSA). Molecules with a TPSA greater than approximately 140 Å^2 are likely to have a low capacity for penetrating cell membranes, while those with PSA ≤ 60 Å^2 typically have good passive permeability properties.[43] The calculated TPSA for the free sugar disaccharides **9** and **10** is 229 Å^2, which is well above the upper limit for good passive membrane diffusion, while for monosaccharides **6**−**8**, the calculated values are somewhat lower (150−167 Å^2) but are also above the upper 140 Å^2 limit, Table 4. For the acetylated compounds **1**−**5**, the calculated TPSAs range from 174 Å^2 (monosaccharide sulfonamide) to 271 Å^2 (disaccharide sulfonamide), again

Table 5. Physicochemical Properties Relevant to Passive Membrane Diffusion with Anomeric Sulfonamides **1**−**10** and the Standard CA Inhibitors Acetazolamide and Topiramate

Compound	Physicochemical properties				
	structure	Molecular weight	cLog P[a]	TPSA (Å^2)[a]	P_e (10^{-6} cm s^{-1})
acetazolamide	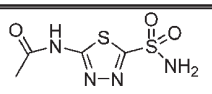	222.2	-1.0	114	<0.15[c]
topiramate	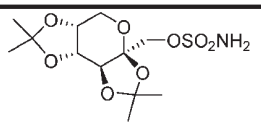	339.4	+0.04	116	0.54 ±0.04[b]
1	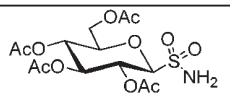	411.4	-0.6	175	<0.1 [c,d]
2	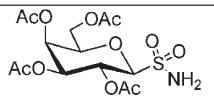	411.4	-0.6	175	-
3	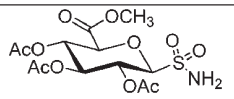	397.4	-1.0	175	-
4	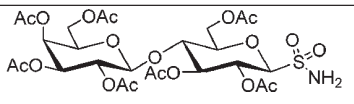	699.6	-0.2	272	-
5	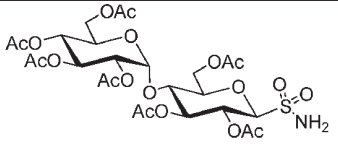	699.6	-0.2	272	<0.02[c]
6	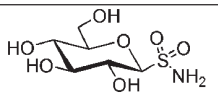	243.2	-2.8	150	<0.4[c]
7	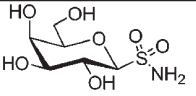	243.2	-2.8	150	-
8	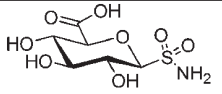	257.2	-3.3	167	-
9	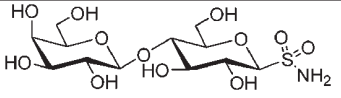	405.4	-5.0	229	-
10	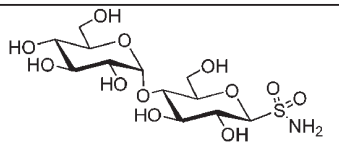	405.4	-5.0	229	<0.5[c]

[a] cLog P and TPSA data calculated using ChemBioDraw Ultra 11.0. [b] Value is represented as mean ± SD (n = 4 wells). [c] The concentration of test compound in the acceptor chamber was lower than the LLQ. Upper limits for the P_e values were estimated using the respective analytical LLQ values as the maximum concentration in the acceptor chamber. [d] During the course of the experiment, some degradation (~35%) of the compound occurred.

well above the threshold for good passive diffusion, Table 5.

Permeability measurements through artificial lipid membrane biolayers have been extensively used to classify small molecules for their passive membrane permeability characteristics, thereby providing an experimental indicator for drug permeability that complements cLog P and TPSA values.[44−47] The technique provides a measurement for apparent in vitro effective permeability (P_e); high permeability compounds typically have P_e values in excess of 3×10^{-6} cm s^{-1}, while low permeability compounds typically have P_e values less than 3×10^{-6} cm s^{-1}.[48,49] The P_e of per-*O*-acetylated anomeric sulfonamides (1 and 5), fully deprotected anomeric sulfonamides (6 and 10), topiramate, acetazolamide, and control compounds were determined using a parallel artificial membrane permeability assay (PAMPA).[45−47] The

experimentally determined P_e values for control compounds, naldolol and verapamil, representing low and high membrane permeability markers, respectively, were used to confirm suitable permeability properties of the membranes. The experimental values of P_e at pH 7.4 using the PAMPA assay are given in Table 5. The only compound for which a measurable concentration was observed in the acceptor compartment was topiramate, with a P_e of 0.54 ($\pm$0.04) $\times$ 10^{-6} cm s^{-1}. On the basis of the permeability classification criteria, the permeability of topiramate across the PAMPA lipid membrane is low or poor. For the other compounds tested, including acetazolamide and the test compounds, the concentrations in the acceptor chamber were below the analytical lower limits of quantitation (LLQ), suggesting that these compounds have very low permeability in this assay. A theoretical estimate of the maximum P_e value for each compound was calculated using the respective LLQ values, Table 4. The PAMPA results for **1**, **5**, **6**, and **10** as representative anomeric sulfonamides (that include an example of monosaccharide, disaccharide, sugar−OAc and sugar−OH) confirm that this class of compound would be expected to have poor passive membrane permeability. This characteristic of the molecules is expected to lead to preferential inhibition of the transmembrane CAs IX and XII over cytosolic CAs, however further in vivo studies are required to confirm this hypothesis.

Conclusions

It has been widely acknowledged that physicochemical properties must be addressed at the onset of a drug discovery campaign so that early candidates have enhanced drug-like profiles. New oncology drugs are desperately needed, and medicinal chemistry must capitalize on any small molecule design avenues available so as to develop safe and efficacious therapeutics that selectively target and kill cancer cells. To maximize the benefits of future chemotherapies involving CA inhibition as part of a cancer treatment regime, it will be essential to develop compounds that specifically target the extracellular domains of the relevant CAs. Selective inhibition among isozymes is a challenging hurdle in the drug discovery process, and for the CA enzyme family, the highly conserved active site structure and topology has made it difficult to target subtle isozyme differences by rational drug design. Herein we have explored an alternate strategy toward CA isozyme selectivity that takes into account the relevant biological landscape for both normal and cancerous cells or tissues associated with CAs. Our approach has been to target the extracellular domains of CA enzymes involved in cancer by the design of compound structures and properties that impart poor membrane permeability. Such compounds may prove to be desirable for chemotherapy if delivered through a route of drug administration other than oral.

Specifically, we have presented a new class of CA inhibitor comprising of *S*-glycosyl primary sulfonamides (**1**−**10**). The aromatic moiety of the classical zinc binding sulfonamide CA inhibitors is absent from these compounds and instead they incorporate a hydrophilic mono- or disaccharide fragment directly attached to the sulfonamide group. We have investigated the membrane permeability properties of the carbohydrate-based CA inhibitors and confirm that these compounds have poor passive membrane permeability and hence are positioned to selectively target extracellular CA active sites in the in vivo context. Protein X-ray crystallography structures for three anomeric sulfonamides as well as the sugar sulfamate, topiramate, were obtained in complex with hCA II, and results have provided an extensive insight into the ligand-active site molecular recognition attributes that will guide the future development of this class of compound as CA inhibitors. For example, the attachment of appropriate moieties to modify the overall shape of the ligands to enable more direct interactions with active site protein residues and enhance enzyme inhibition while retaining the membrane impermeability and drug lead-like properties of the compounds presented will be undertaken.

Experimental Section

Chemistry. The syntheses of compounds **1**−**10** were prepared as previously described by ourselves.[21] All reagents were purchased from Sigma-Aldrich Chemical Company with the exception of methyl 1,2,3,4-tetra-*O*-acetyl-β-D-glucopyranuronate, which was synthesized as described in the literature.[50] All reactions were monitored by TLC using Merck $F60_{254}$ silica plates visualized with UV light (λ = 254 nm), sulphuric acid stain (5% H_2SO_4 in ethanol), and/or orcinol stain (1 g of orcinol monohydrate in a mixture of EtOH:H_2O:H_2SO_4 72.5:22.5:5). Silica gel flash chromatography was performed on Davisil silica gel 60 Å (230−400 mesh). Reverse phase chromatography was performed using Phenomenex C-18 silica prepacked cartridges and eluted with a gradient of H_2O−MeOH (from 100:0 to 0:100). NMR (^{1}H, ^{13}C {^{1}H}, gCOSY, and HSQC) spectra were recorded on a Varian 500 MHz spectrometer at room temperature. For ^{1}H and ^{13}C NMR run in $CDCl_3$, chemical shifts (δ) are reported in ppm relative to the solvent residual peak: proton (δ = 7.27 ppm) and carbon (δ = 77.2 ppm). Chemical shifts for ^{1}H and ^{13}C NMR run in DMSO-d_6 are reported in ppm relative to residual solvent proton (δ = 2.50 ppm) and carbon (δ = 39.5 ppm) signals, respectively. For ^{1}H NMR run in D_2O, chemical shifts are reported in ppm relative to the solvent residual peak: proton (δ = 4.80 ppm). Multiplicity is indicated as follows: s (singlet), d (doublet), t (triplet), m (multiplet), dd (doublet of doublet), ddd (doublet of doublet of doublet), br s (broad singlet). Coupling constants are reported in hertz (Hz). Melting points are uncorrected. Low resolution mass spectra were acquired in positive ion mode on an Applied Biosystems Pty Ltd. Mariner ESI-TOF mass spectrometer. High resolution mass spectra were performed in positive ion mode on an Apex III Bruker Daltonics 4.7T Fourier transform mass spectrometer (FTMS) fitted with an Apollo electrospray ionization source. All MS analysis samples were prepared as solutions in methanol. Optical rotations were measured on a Jasco P-1020 polarimeter at 25 °C with Na-589 nm wavelength and reported as an average of 10 measurements. The purities of isolated products were determined by HPLC obtained on an LCMS instrument (MS-ZQ Waters; HPLC-Alliance Waters) using a HPLC column (Ascentis, C18 3 μm, 5 cm $\times$ 4.6 mm). Elution was performed with a gradient of water:methanol (containing 1% formic acid) from 95:5 to 0:100 for 10 min at a flow rate of 1 mL/min. UV (200 to 400 nm) and evaporative light scattering detection (ELSD-Alltech) detection were used. Purity of all compounds proved to be ≥95%.

Carbonic Anhydrase Catalytic Inhibition Assay. An SX. 18MV-R Applied Photophysics stopped-flow instrument has been used for assaying the CA I, II, IX, and XII CO_2 hydration activity.[23] Phenol red (at a concentration of 0.2 mM) has been used as indicator, working at the absorbance maximum of 557 nm, with 10 mM Hepes (pH 7.5) as buffer, 0.1 M $NaClO_4$ (for maintaining constant the ionic strength−this anion is not inhibitory), following the CA-catalyzed CO_2 hydration reaction for a period of 10−100 s. Saturated CO_2 solutions in water at 20 °C were used as substrate. Stock solutions of inhibitors were prepared at a concentration of 10−50 mM (in the assay buffer) and dilutions up to 1 nM done with the assay buffer mentioned above. Inhibitor and enzyme solutions were preincubated together for 15 min at room temperature prior to assay in order to

allow for the formation of the E−I complex. The inhibition constants were obtained by nonlinear least-squares methods using PRISM 3. The curve-fitting algorithm allowed us to obtain the IC_{50} values, working at the lowest concentration of substrate of 1.7 mM), from which K_i values were calculated by using the Cheng−Prusoff equation. The catalytic activity (in the absence of inhibitors) of these enzymes was calculated from Lineweaver−Burk plots and represent the mean from at least three different determinations. Enzyme concentrations were 10.3 nM for CA I and CA II, 12 nM for CA IX, and 15 nM for hCA XII. Kinetic parameters and inhibition constants were calculated as described previously.[11,51] Enzymes used here were recombinant ones, prepared and purified as described earlier.[11,51]

Protein X-ray Crystallography. Human recombinant CA II was expressed in *Escherichia coli* BL21(DE3) using autoinduction[52] as implemented in our laboratory. Soluble protein was purified by anion exchange chromatography using Q-Sepharose resin. The concentrated protein was subjected to cocrystallization with ligands, using a selection of ammonium sulfate containing conditions from our in-house factorial collection (2.6 or 2.9 M $(NH_4)_2SO_4$ buffered with either 0.1 M TRIS pH 8.0, 0.1 M TRIS pH 8.5, or 0.1 M glycine pH 9.5). Crystallization droplets were constituted by mixing 3 μL of protein stock solution (18 mg mL^{-1} in 100 mM NaCl, 20 mM HEPES, pH 8.0), with 2 μL reservoir, and 1 μL of ligand solution (60 mM in MeOH) solution. The final concentration of protein in the droplets was 9 mg mL^{-1}; the molar ratio of ligand to protein was 33. X-ray diffraction data was obtained under cryoconditions at the in-house diffractometer (Rigaku MM007-HF with an R-Axis IV++ detector), as well as the Australian Synchrotron beamline PX1 equipped with a Quantum ADSC CCD detector. Data were processed using Mosflm[53] or XDS[54] and the CCP4 suite.[55] All crystals belonged to the monoclinic space group $P2_1$, and CA II:ligand complex structures were determined by difference Fourier techniques using the structure of human CA II (PDB code 1CA2). The ligand-bound structures were refined using CNS[56] with ligand topologies generated by PRODRG.[57] Manual model building and visual inspection was performed using the programs O[58] and Coot.[59] Refined structures were checked for acceptable geometry using PROCHECK,[60] and the Ramachandran plot showed no residues in the disallowed regions. Coordinates and structure factors have been deposited with the PDB (accession codes: 3HKN, 3HKQ, 3HKT, and 3HKU for hCA II complexes with **4**, **7**, **10**, and topiramate).

Homology Modeling. Secondary structure elements of hCA IX were predicted using PSIPRED,[61] and a structure-based sequence alignment of the catalytic subunit of hCA IX with hCA XII (PDB: 1JD0) was generated manually. Twenty independent homology models were computed with MODELER,[62] and that with the lowest energy was selected. The overall geometry was scrutinized with PROCHECK,[60] and models were visually inspected with O.[58]

Membrane Permeability Studies. The apparent in vitro effective permeability (P_e) of per-*O*-acetylated anomeric sulfonamides (**1** and **5**), fully deprotected anomeric sulfonamides (**6** and **10**), topiramate, and acetazolamide were determined using a parallel artificial membrane permeability assay (PAMPA).[45−47] Standard 96-well PVDF filter plates were coated with a solution of lipid material (dioleoyl-3-phosphocholine (DOPC)) to prepare the artificial membrane. The filter plate was sandwiched with a 96-well acceptor plate filled with transport buffer (Hanks balanced salt solution containing 20 mM HEPES, pH 7.4). The solubility of each test compound in the transport buffer at the donor concentration was confirmed prior to the experiment. For topiramate, acetazolamide, **1**, and **5**, donor solutions (20 μM) were prepared in transport buffer and quadruplicate aliquots (200 μL) transferred to the donor wells. For **6** and **10**, a donor concentration of 200 μM was used owing to the poor analytical sensitivities for these compounds using the LCMS assay. The acceptor compartment was filled with 300 μL of blank transport buffer. Compounds were allowed to permeate across the artificial membrane for 4 h at 37 °C with 200 rpm orbital shaking, after which the sandwich was separated and samples from the donor and acceptor wells transferred into a fresh 96-well plate for analysis. Control compounds, nadolol and verapamil, representing low and high membrane permeability markers, respectively, were included in the PAMPA plate. To monitor for membrane integrity, 20 μM nadolol (a low permeability marker) was added to all wells concurrently with the test compound. Compound stability in transport buffer at 37 °C (4 h) was also assessed. All samples were quenched with an equal volume of acetonitrile, and the concentrations of test and control compounds were quantitated by LC-MS using ESI-positive ion mode. The lower limits of quantitation (LLQ) were found to be 0.005 μM (**1**, **5**, topiramate), 0.05 μM (acetazolamide), and 1 μM (**6**, **10**). The effective permeability coefficient (P_e) of each compound was calculated as described previously.[46]

Acknowledgment. This work was financed in part by the Australian Research Council (grant no. DP0877554 to S.-A.P. and S.C.), Griffith University, an EU grant of the 6th framework programme (DeZnIT project to C.T.S.), and an EU grant of the 7th framework programme (METOXIA project to C.T.S.). We thank A/Prof. Jean-Yves Winum for the sample of topiramate used in this study. cDNA for hCA II was kindly provided by Prof. Carol Fierke, University of Michigan. A.H. acknowledges the award of beam time by the Australian Synchrotron and on-site support by Trevor Huyton.

References

(1) For recent reviews of carbonic anhydrases see: Supuran, C. T. Carbonic anhydrases: novel therapeutic applications for inhibitors and activators. *Nat. Rev. Drug Discovery* **2008**, *7*, 168–181. (b) Krishnamurthy, V. M.; Kaufman, G. K.; Urbach, A. R.; Gitlin, I.; Gudiksen, K. L.; Weibel, D. B.; Whitesides, G. M. Carbonic Anhydrase as a Model for Biophysical and Physical-Organic Studies of Proteins and Protein Ligand Binding. *Chem. Rev*. **2008**, *108*, 946–1051.

(2) Lipinski, C.; Hopkins, A. Navigating chemical space for biology and medicine. *Nature* **2004**, 855–861.

(3) Marquis, R. E.; Whitson, J. T. Management of glaucoma: focus on pharmacological therapy. *Drugs Aging* **2005**, *22*, 1–21.

(4) Sugrue, M. F. Pharmacological and ocular hypotensive properties of topical carbonic anhydrase inhibitors. *Prog. Retinal Eye Res*. **2000**, *19*, 87–112.

(5) Svastova, E.; Hulikova, A.; Rafajova, M.; Zatovicova, M.; Gibadulinova, A.; Casini, A.; Cecchi, A.; Scozzafava, A.; Supuran, C. T.; Pastorek, J.; Pastoreková, S. Hypoxia activates the capacity of tumor-associated carbonic anhydrase IX to acidify extracellular pH. *FEBS Lett*. **2004**, *577*, 439–445.

(6) Chiche, J.; Ilc, K.; Laferriére, J.; Trottier, E.; Dayan, F.; Mazure, N. M.; Brahimi-Horn, M. C.; Pouysségur, J. Hypoxia-inducible carbonic anhydrase IX and XII promote tumor cell growth by counteracting acidosis through the regulation of the intracellular pH. *Cancer Res*. **2009**, *69*, 358–368.

(7) Swietach, P.; Vaughan-Jones, R. D.; Harris, A. L. Regulation of tumor pH and the role of carbonic anhydrase 9. *Cancer Metastasis Rev*. **2007**, *26*, 299–310.

(8) Wykoff, C. C.; Beasley, N. J. P.; Watson, P. H.; Turner, K. J.; Pastorek, J.; Sibtain, A.; Wilson, G. D.; Turley, H.; Talks, K. L.; Maxwell, P. H.; Pugh, C. W.; Ratcliffe, P. J.; Harris, A. L. Hypoxia-inducible regulation of tumor-associated carbonic anhydrases. *Cancer Res*. **2000**, *60*, 7075–7083.

(9) Thiry, A.; Dogné, J. M.; Masereel, B.; Supuran, C. T. Targeting tumor-associated carbonic anhydrase IX in cancer therapy. *Trends Pharmacol. Sci*. **2006**, *27*, 566–573.

(10) Vullo, D.; Franchi, M.; Gallori, E.; Pastorek, J.; Scozzafava, A.; Pastorekova, S.; Supuran, C. T. Carbonic anhydrase inhibitors. Inhibition of the tumor-associated isozyme IX witharomatic and heterocyclic sulfonamides. *Bioorg. Med. Chem. Lett*. **2003**, *13*, 1005–1009.

(11) Vullo, D.; Innocenti, A.; Nishimori, I.; Pastorek, J.; Scozzafava, A.; Pastoreková, S.; Supuran, C. T. Carbonic anhydrase inhibitors. Inhibition of the transmembrane isozyme XII with sulfonamides—a new target for the design of antitumor and antiglaucoma drugs? *Bioorg. Med. Chem. Lett*. **2005**, *15*, 963–969.
(12) Winum, J.-Y.; Poulsen, S.-A.; Supuran, C. T. Therapeutic applications of glycosidic carbonic anhydrase inhibitors. *Med. Res. Rev*. **2009**, *29*, 419–435.
(13) Singer, M.; Lopez, M.; Bornaghi, L. F.; Innocenti, A.; Vullo, D.; Supuran, C. T.; Poulsen, S.-A. Inhibition of carbonic anhydrase isozymes with benzene sulfonamides incorporating thio, sulfinyl and sulfonyl glycoside moieties. *Bioorg. Med. Chem. Lett*. **2009**, *19*, 2273–2276.
(14) Wilkinson, B. L.; Innocenti, A.; Vullo, D.; Supuran, C. T.; Poulsen, S.-A. Inhibition of carbonic anhydrases with glycosyltriazole benzene sulfonamides. *J. Med. Chem*. **2008**, *51*, 1945–1953.
(15) Wilkinson, B. L.; Bornaghi, L. F.; Houston, T. A.; Innocenti, A.; Vullo, D.; Supuran, C. T.; Poulsen, S.-A. Carbonic anhydrase inhibitors: inhibition of isozymes I, II and IX with triazole-linked *O*-glycosides of benzene sulfonamides. *J. Med. Chem*. **2007**, *50*, 1651–1657.
(16) Wilkinson, B. L.; Bornaghi, L. F.; Houston, T. A.; Innocenti, A.; Vullo, D.; Supuran, C. T.; Poulsen, S.-A. Inhibition of membrane-associated carbonic anhydrase isozymes IX, XII and XIV with a library of glycoconjugate benzenesulfonamides. *Bioorg. Med. Chem. Lett*. **2007**, *17*, 987–992.
(17) Wilkinson, B. L.; Bornaghi, L. F.; Houston, T. A.; Innocenti, A.; Supuran, C. T.; Poulsen, S.-A. A novel class of carbonic anhydrase inhibitors: glycoconjugate benzene sulfonamides prepared by "click-tailing". *J. Med. Chem*. **2006**, *49*, 6539–6548.
(18) Aich, U.; Campbell, C. T.; Elmouelhi, N.; Weier, C. A.; Sampathkumar, S.-G.; Choi, S. S.; Yarema, K. J. Regioisomeric SCFA attachment to hexosamines separates metabolic flux from cytotoxicity and MUC 1 suppression. *ACS Chem. Biol*. **2008**, *3*, 230–240.
(19) Elmouelhi, N.; Aich, U.; Paruchuri, V. D. P.; Meledeo, M. A.; Campbell, C. T.; Wang, J. J.; Srinivas, R.; Khanna, H. S.; Yarema, K. J. Hexosamin template. A platform for modulating gene expression and for sugar-based drug discovery. *J. Med. Chem*. **2009**, *52*, 2515–2530.
(20) Meutermans, W.; Le, G. T.; Becker, B. Carbohydrates as scaffolds in drug discovery. *ChemMedChem* **2006**, *1*, 1164–1194.
(21) Lopez, M.; Drillaud, N.; Bornaghi, L. B.; Poulsen, S.-A. Synthesis of *S*-glycosyl primary sulfonamides. *J. Org. Chem*. **2009**, *74*, 2811–2816.
(22) Czifrák, K.; Somsák, L. Synthesis of anomeric sulfonamides and their behavior under radical-mediated bromination conditions. *Carbohydr. Res*. **2009**, *344*, 269–277.
(23) Khalifah, R. G. T. The carbon dioxide hydration activity of carbonic anhydrase. *J. Biol. Chem*. **1971**, *246*, 2561–2573.
(24) Winum, J.-Y.; Scozzafava, A.; Montero, J.-L.; Supuran, C. T. New zinc binding motifs in the design of selective carbonic anhydrase inhibitors. *Mini Rev. Med. Chem*. **2006**, *6*, 921–936.
(25) Casini, A.; Antel, J.; Abbate, F.; Scozzafava, A.; David, S.; Waldeck, H.; Schafer, S.; Supuran, C. T. Carbonic anhydrase inhibitors: SAR and X-ray crystallographic study for the interaction of sugar sulfamates/sulfamides with isozymes I, II and IV. *Bioorg. Med. Chem. Lett*. **2003**, *13*, 841–845.
(26) Winum, J.-Y.; Scozzafava, A.; Montero, J.-L.; Supuran, C. T. Sulfamates and their therapeutic potential. *Med. Res. Rev*. **2005**, *25*, 186–228.
(27) Winum, J.-Y.; Scozzafava, A.; Montero, J.-L.; Supuran, C. T. The sulfamide motif in the design of enzyme inhibitors. *Expert Opin. Ther. Pat*. **2006**, *16*, 27–47.
(28) Winum, J.-Y.; Scozzafava, A.; Montero, J.-L.; Supuran, C. T. Therapeutic potential of sulfamides as enzyme inhibitors. *Med. Res. Rev*. **2006**, *26*, 767–792.
(29) Winum, J.-Y.; Temperini, C.; El Cheikh, K.; Innocenti, A.; Vullo, D.; Ciattini, S.; Montero, J.-L.; Scozzafava, A.; Supuran, C. T. Carbonic anhydrase inhibitors: clash with Ala65 as a means for designing inhibitors with low affinity for the ubiquitous isozyme II, exemplified by the crystal structure of the topiramate sulfamide analogue. *J. Med. Chem*. **2006**, *49*, 7024–7031.
(30) Shank, R. P.; Maryanoff, B. E. Molecular pharmacodynamics, clinical yherapeutics, and pharmacokinetics of topiramate. *CNS Neurosci. Ther*. **2008**, *14*, 120–142.
(31) Maryanoff, B. E. Pharmacutical "gold" from neurostabilizing agents: Topiramate and successor molecules. *J. Med. Chem*. **2009**, *52*, 3431–3440.
(32) De Simone, G.; Di Fiore, A.; Menchise, V.; Pedone, C.; Antel, J.; Casini, A.; Scozzafava, A.; Wurl, M.; Supuran, C. T. Carbonic anhydrase inhibitors. Zonisamide is an effective inhibitor of the cytosolic isozyme II and mitochondrial isozyme V: solution and X-ray crystallographic studies. *Bioorg. Med. Chem. Lett*. **2005**, *15*, 2315–2320.
(33) Genis, C.; Sippel, K. H.; Case, N.; Cao, W.; Avvaru, B. S.; Tartaglia, L. J.; Govindasamy, L.; Tu, C.; Agbandje-McKenna, M.; Silverman, D. N.; Rosser, C. J.; McKenna, R. Design of a carbonic anhydrase IX active-site mimic to screen inhibitors for possible anticancer properties. *Biochemistry* **2009**, *48*, 1322–1331.
(34) Hofmann, A.; Wlodawer, A. PCSB—a program collection for structural biology and biophysical chemistry. *Bioinformatics* **2002**, *18*, 209–210.
(35) DeLano, W. *The PyMOL Molecular Graphics System*; **2002**; http://www.pymol.org.
(36) Hartshorn, M. J. AstexViewer: A visualisation aid for structure-based drug design. *J. Comput.-Aided. Mol. Des*. **2002**, *16*, 871–881.
(37) Scozzafava, A.; Menabuoni, L.; Mincione, F.; Supuran, C. T. Carbonic anhydrase inhibitors. A general approach for the preparation of water-soluble sulfonamides incorporating polyamino-polycarboxylate tails and of their metal complexes possessing long-lasting, topical intraocular pressure-lowering properties. *J. Med. Chem*. **2002**, *45*, 1466–1476.
(38) Vullo, D.; Steffansen, B.; Brodin, B.; Supuran, C. T.; Scozzafava, A.; Nielsen, C. U. Carbonic anhydrase inhibitors: transepithelial transport of thioureido sulfonamide inhibitors of the cancer-associated isozyme IX is dependent on efflux transporters. *Bioorg. Med. Chem*. **2006**, *14*, 2418–2427.
(39) Scozzafava, A.; Briganti, F.; Ilies, M. A.; Supuran, C. T. Carbonic anhydrase inhibitors: synthesis of membrane-impermeant low molecular weight sulfonamides possessing in vivo selectivity for the membrane-bound versus cytosolic isozymes. *J. Med. Chem*. **2000**, *43*, 292–300.
(40) Pastorekova, S.; Casini, A.; Scozzafava, A.; Vullo, D.; Pastorek, J.; Supuran, C. T. Carbonic anhydrase inhibitors: The first selective, membrane—impermeant inhibitors targeting the tumor-associated isozyme IX. *Bioorg. Med. Chem. Lett*. **2004**, *14*, 869–873.
(41) Rami, M.; Cecchi, A.; Montero, J.-L.; Innocenti, A.; Vullo, D.; Scozzafava, A.; Winum, J.-Y.; Supuran, C. T. Carbonic anhydrase inhibitors: design of membrane-impermeant copper(II) complexes of DTPA-, DOTA-, and TETA-tailed sulfonamides targeting the tumor-associated transmembrane isoform IX. *ChemMedChem* **2008**, *3*, 1780–1788.
(42) Kerns, E. H.; Di, L. *Drug-Like Properties: Concepts, Structure Design and Methods: From ADME to Toxicity Optimization*, 1st ed.; Academic Press: London, 2008; pp 43−47.
(43) Palm, K.; Stenberg, P.; Luthman, K.; Artursson, P. Polar molecular surface properties predict the intestinal absorption of drugs in humans. *Pharm. Res*. **1997**, *14*, 568–571.
(44) Kerns, E. H.; Di, L. *Drug-Like Properties: Concepts, Structure Design and Methods: From ADME to Toxicity Optimization*; 1st ed.; Academic Press: London, 2008; pp 287−298.
(45) Kansy, M.; Senner, F.; Gubernator, K. Physicochemical high throughput screening: parallel artificial membrane permeation assay in the description of passive absorption processes. *J. Med. Chem*. **1998**, *41*, 1007–1010.
(46) Avdeef, A. Physicochemical profiling (solubility, permeability and charge state). *Curr. Top. Med. Chem*. **2001**, *1*, 277–351.
(47) Wohnsland, F.; Faller, B. High-throughput permeability pH profile and high-throughput alkane/water log P with artificial membranes. *J. Med. Chem*. **2001**, *44*, 923–930.
(48) Zhu, C.; Jiang, L.; Chen, T.-M.; Hwang, K.-K. A comparative study of artificial membrane permeability assay for high throughput profiling of drug absorption potential. *Eur. J. Med. Chem*. **2002**, *37*, 399–407.
(49) *FDA Guidance for Industry 2000: Waiver of In Vivo Bioavailability and Bioequivalence Studies for Immediate-Release Solid Oral Dosage Forms Based on a Biopharmaceutics Classification System*; U.S. Food and Drug Adminstration, **2000**.
(50) Nakajima, R.; Ono, M.; Aiso, S.; Akita, H. Synthesis of methyl-1-*O*-(4-hydroxymethamphetaminyl)-α-D-glucopyranuronate. *Chem. Pharm. Bull* **2005**, *53*, 684.
(51) Winum, J.-Y.; Vullo, D.; Casini, A.; Montero, J.-L.; Scozzafava, A.; Supuran, C. T. Carbonic anhydrase inhibitors: Inhibition of transmembrane, tumor-associated isozyme IX, and cytosolic isozymes I and II with aliphatic sulfamates. *J. Med. Chem*. **2003**, *46*, 5471.
(52) Studier, F. Protein production by auto-induction in high density shaking cultures. *Protein Expr. Purif*. **2005**, *41*, 207–234.
(53) Leslie, A. Recent changes to the MOSFLM package for processing film and image plate data. *Joint CCP4 + ESF-EAMCB Newsletter on Protein Crystallography* **1992**, 26.

(54) Kabsch, W. Automatic processing of rotation diffraction data from crystals of initially unknown symmetry and cell constants. *J. Appl. Crystallogr*. **1993**, *26*, 795–800.
(55) Collaborative Computational Project Number 4. The CCP4 suite: programs for protein crystallography. *Acta Crystallogr., Sect. D: Biol. Crystallogr*. **1994**, *50*, 760−763.
(56) Brunger, A.; Adams, P.; Clore, G.; Delano, W.; Gros, P.; Grosse-Kunstleve, R.; Jiang, J.; Kuszewski, J.; Nilges, N.; Pannu, N.; Read, R.; Rice, L.; Simonson, T.; Warren, G. Crystallography and NMR system (CNS): a new software system for macromolecular structure determination. *Acta Crystallogr., Sect. D: Biol. Crystallogr*. **1998**, *54*, 905–921.
(57) Schuettelkopf, A. W.; van Aalten, D. M. F. PRODRG—a tool for high-throughput crystallography of protein−ligand complexes. *Acta Crystallogr., Sect. D: Biol. Crystallogr*. **2004**, *60*, 1355–1363.
(58) Jones, T. A.; Zou, J. Y.; Cowan, S.; Kjeldgaard, M. Improved methods for building protein models in electron density maps and location of errors in these models. *Acta Crystallogr., Sect. A: Found. Crystallogr*. **1991**, *47*, 110–119.
(59) Emsley, P.; Cowton, K. Coot: Model-Building Tools for Molecular Graphics. *Acta Crystallogr., Sect. D: Biol. Crystallogr*. **2004**, *60*, 2126–2132.
(60) Laskowski, R.; MacArthur, M.; Moss, D.; Thornton, J. PROCHECK: a program to check the stereochemical quality of protein structures. *J. Appl. Crystallogr*. **1993**, *26*, 283–291.
(61) Bryson, K.; McGuffin, L. J.; Marsden, R. L.; Ward, J. J.; Sodhi, J. S.; Jones, D. T. Protein structure prediction servers at University College London. *Nucleic Acids Res*. **2005**, *33*, W36–W38.
(62) Sali, A.; Blundell, T. Comparative protein modelling by satisfaction of spatial restraints. *J. Mol. Biol*. **1993**, *234*, 779–815.